Thermodynamic Stability of Zimmerman Self-Assembled Dendritic Supramolecules from Atomistic Molecular Dynamics Simulations

Shiang-Tai Lin, Seung Soon Jang, Tahir Çağın, and William A. Goddard, III*

Materials and Process Simulation Center, Beckman Institute, 139-74, California Institute of Technology, Pasadena, California 91125

Received: December 19, 2003; In Final Form: April 26, 2004

We have used the vibrational density of state (DoS) derived from classical molecular dynamic (MD) simulations to investigate the origin of the generation-dependent stability of the hydrogen-bond-mediated self-assembly of supramolecular dendritic structures synthesized and characterized by Zimmerman and co-workers. In this method, the DoS distribution is calculated from the Fourier transform of the velocity autocorrelation function, and the thermodynamic properties are determined by weighting each vibrational mode with the harmonic oscillator statistics. Our simulation results confirm the experimental findings that circular and linear configurations may coexist at lower generations but that only circular forms are stable at higher generations. From analyzing the free energy extracted from the MD on both linear and hexagonal forms of the first through fourth generation dendrimers, we find that *entropic* contributions dominate the stability of these self-assembled systems. This method provides additional detailed information on the thermodynamic properties of suprastructures, which should be useful in the study of other complex systems such as proteins and DNA.

1. Introduction

Self-assembled supramolecules, such as DNA,[1] hemoglobin,[2] ribosomes,[3] etc., are ubiquitously observed in living organisms and play an essential role in their various functions and mechanisms. These complicated and large-scale biomolecular systems often consist of many replicas of somewhat simple constitutional subunits (monomers). Interestingly, the structures of these giant molecules can be stabilized through *noncovalent* interactions between the monomers such as electrostatic, van der Waals, and hydrogen bond interactions. These noncovalent interactions impart reversibility to the self-organization of monomers. In other words, a specific self-assembled supramolecular structure can exist stably under one specific condition, but not under others, and whenever that condition is recovered, so is the supramolecular structure. Through the control of environmental conditions such as pH values and ionic strength in solution, the suprastructures may undergo dramatic changes because the equilibrium state may shift to another point. Of particular interest are hydrogen-bond-mediated systems whose suprastructures can be controlled through the choice of apolar, aprotic, or aqueous solvents. It is worth noting that the characteristic properties exhibited in these self-assembled systems are not necessarily the same as the intrinsic properties observed in their monomeric units. Therefore, many efforts have been made so far not only to understand these self-assembled systems in nature but also to mimic them using synthetic monomeric units to obtain some desirable functions.[4−15] However, in order to design new structures with novel properties and functions, it is essential to have a good understanding of the underlying thermodynamic principles that govern the stability of the self-assembled supramolecular structures. To the best of our knowledge, however, a full thermodynamic explanation including entropy has not been available yet to estimate the stability of self-assembled supramolecular structures. It is still a great challenge to determine the thermodynamic origin of the structural stability observed in experiments. Once we can quantify and predict the thermodynamic properties such as enthalpy and entropy that govern the stability of a supramolecular structure, the design of a chemical structure for monomers that leads to a desirable suprastructure and functions would become possible.

New advances in simulation techniques, improvements in computing power, and fast and efficient parallel computing algorithms make it feasible to study giant size self-assemblies by molecular level simulation and modeling methods with high accuracy within a reasonable time. In this paper, we demonstrate the use of classical molecular dynamics (MD) simulation to determine the stability of the hydrogen-bond-driven dendrimers (Figure 1) first synthesized by Zimmerman and co-workers.[16] The core part (Figure 1a) of such dendrimers contains four carboxylic acid groups that allow the dendrimer to self-assemble in apolar organic solvents, such as dichloromethane and chloroform, and form either circular hexamers (Figure 1b) or linear aggregates (Figure 1c). Results from size exclusion chromatography (SEC) for various dendrimer concentrations in dichloromethane solution suggest that the linear aggregate exists only for generation 1 and the circular hexamer is the dominant form for generations 2−4. Such generation-dependent stability of the hydrogen-bond-mediated dendrimer has been attributed to the subtle balance among the favorable hydrogen bond interactions in the core, favorable van der Waals interaction in the dendrons, and unfavorable steric repulsions between neighboring dendrimers.[16] However, to the best of our knowledge, a more detailed analysis on the actual role of the different types of energetic interactions has not yet been done and the entropic effect has not been taken into account.

To investigate the generation-dependent stability of the hydrogen-bond-mediated Zimmerman dendrimer, the free energies are calculated from the classical MD trajectories using the

* To whom correspondence should be addressed. E-mail: wag@wag.caltech.edu.

10.1021/jp037947i CCC: $27.50
Published on Web 06/19/2004

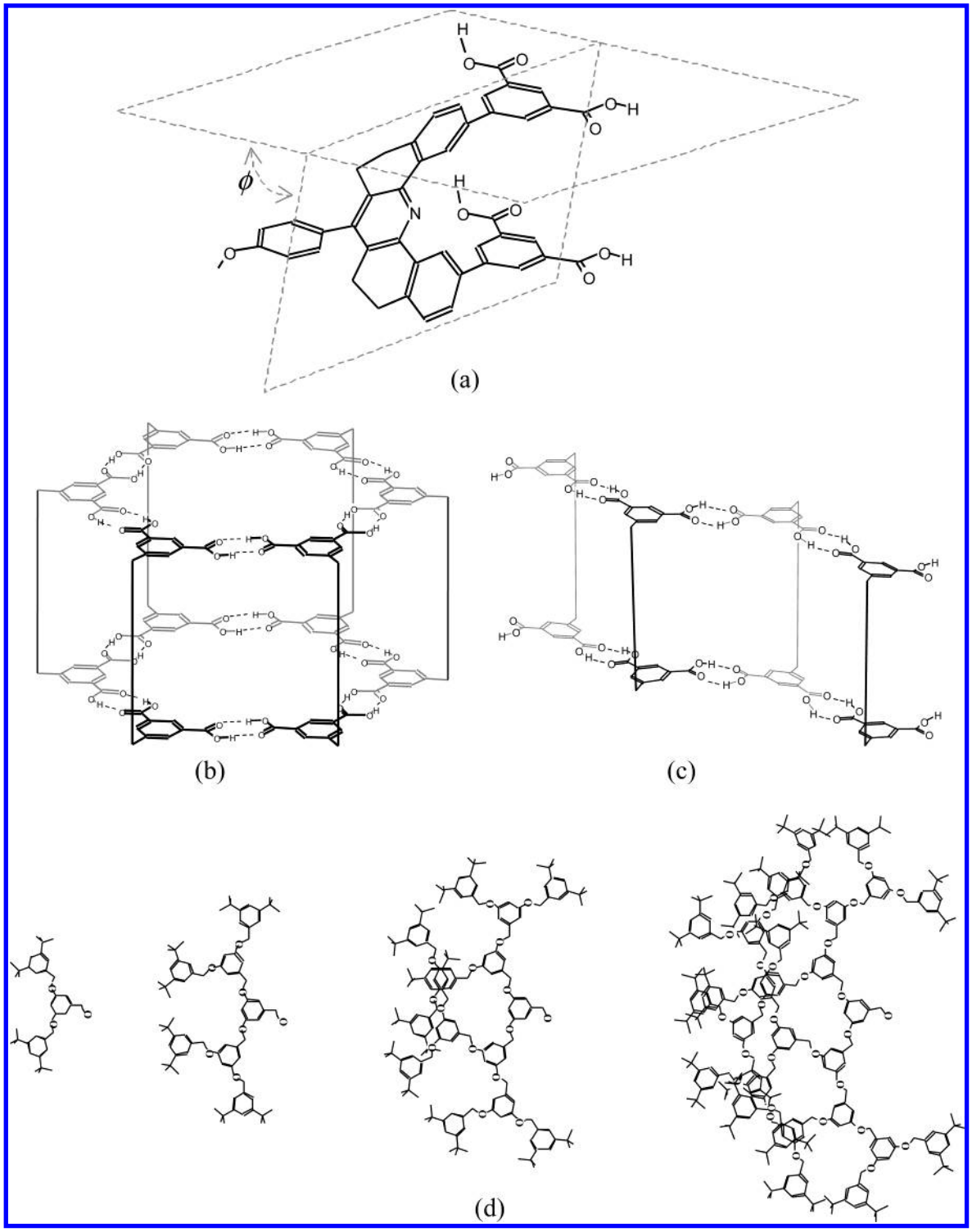

Figure 1. Schematic of the core monomer structure (a), circular hexamer (b), linear-type aggregate (c), and the dendrons (d) for generations 1−4.

velocity spectrum method of Berens et al.[17] which employs the quasi-harmonic approximation. The enthalpic and entropic contributions are determined by applying harmonic quantum statistics to the normal modes calculated via the Fourier transform of the velocity autocorrelation function. This method allows the determination of properties at finite temperatures, therefore, providing rich insight into the thermodynamic origin of the self-assembled dendrimer. In this paper, we focus on the study of the relative stability between the linear and circular type of the hexamer aggregate in vacuum, which may represent the most apolar solvent condition. Under such a condition the harmonic approximation in the velocity spectrum method should be adequate, as other similar methods[18,19] that determine the normal modes from atomic position fluctuations have been shown to provide a good estimate of protein conformational stability. One advantage of using the velocity spectrum method is that in the cases where diffusion becomes important and the harmonic approximation breaks down, the effects from particle diffusion can be rigorously treated and the free energy can be accurately determined.[20] We found that the classical MD energies (kinetic and potential) are not sufficient to explain the generation-dependent stability. The inclusion of an entropic

effect determined from the velocity spectrum method allows a successful description of the relative stability between dendrimers.

2. Thermodynamic Properties of Gas Phase Molecules

Assuming no coupling between translational, rotational, and vibrational motions, the canonical partition function q of a gas molecule can be expressed as the product of its components

$$q(V,T) = q_{trans}(V,T)q_{rot}(T)q_{vib}(T) \tag{1}$$

Thus, the Helmholtz free energy can be decomposed to the corresponding components

$$A = V_0 - kT \ln q = A_{trans} + A_{vib} + A_{rot} \tag{2}$$

where V_0 is the reference energy. Likewise, the total energy E and entropy S are

$$E = kT^2\left(\frac{\partial \ln q}{\partial T}\right) = E_{trans} + E_{vib} + E_{rot} \tag{3}$$

$$S = k \ln q + kT\left(\frac{\partial \ln q}{\partial T}\right) = S_{trans} + S_{vib} + S_{rot} \tag{4}$$

The determination of the components of the partition function and the reference energy is outlined below.

2.1. Translation Partition Function. The translation partition function is

$$q_{trans}(V,T) = \left(\frac{2\pi M}{\beta h^2}\right)^{3/2} V \tag{5}$$

where M is the mass of the molecule, h is Planck's constant, and $\beta = 1/(kT)$.

2.2. Rotation Partition Function. The rotation partition function is determined at the classical limit

$$q_{rot}(T) = \frac{\pi^{1/2}}{\sigma}\left(\frac{8\pi^2 I_A}{\beta h^2}\right)^{1/2}\left(\frac{8\pi^2 I_B}{\beta h^2}\right)^{1/2}\left(\frac{8\pi^2 I_C}{\beta h^2}\right)^{1/2} \tag{6}$$

where σ is the symmetry number of the molecule; I_A, I_B, and I_C are the principal moments of inertia of the molecule.

2.3. Vibration Partition Function. The vibration partition is calculated from the velocity spectrum.[17] In this method, the effective vibration intensity, or density of states $S(\upsilon)$, of a system at a frequency υ can be determined from the Fourier transform of the velocity autocorrelation

$$S(\upsilon) = \frac{2}{kT}\lim_{\tau\to\infty}\int_{-\tau}^{\tau} C(t) \exp(-i2\pi\upsilon t)\, dt \tag{7}$$

where $C(t)$ is the mass-weighted velocity autocorrelation defined as

$$C(t) = \sum_{i=1}^{N}\sum_{j=1}^{3} m_i c_i^j(t) \tag{8}$$

where N is the number of atoms in the system, m_i is the mass of atom i, and $c_i^j(t)$ is the j component ($j = x, y,$ and z) of the velocity autocorrelation of atom i

$$c_i^j(t) = \lim_{\tau\to\infty}\frac{\int_{-\tau}^{\tau} v_i^j(t'+t)v_i^j(t')\, dt'}{\int_{-\tau}^{\tau} dt'} = \lim_{\tau\to\infty}\frac{1}{2\tau}\int_{-\tau}^{\tau} v_i^j(t'+t)v_i^j(t')\, dt' \tag{9}$$

It can be shown that the integration of $S(\upsilon)$ gives the total degrees of freedom of the system, i.e.,

$$\int_0^\infty S(\upsilon)\, d\upsilon = 3N \tag{10}$$

As in most of the molecular dynamics codes, the system translational and/or rotational degrees of freedom are removed in our simulations. For this case, $S(\upsilon)$ is renormalized such that the integration of eq 10 gives the proper total degrees of freedom of the system ($3N - 6$).

Assuming that all the vibrations are independent (uncorrelated) harmonic motions, the vibration partition function q_{vib} of the system can be calculated using that of the quantum harmonic oscillators $q_{HO}^Q(\upsilon)$

$$\ln q_{vib} = \int_0^\infty d\upsilon\, S(\upsilon) \ln q_{HO}^Q(\upsilon) \tag{11}$$

where

$$q_{HO}^Q(\upsilon) = \frac{\exp(-\beta h\upsilon/2)}{1 - \exp(-\beta h\upsilon/2)} \tag{12}$$

The energy E, entropy S, and Helmholtz free energy A of the system can, therefore, be determined as

$$E_{vib} = V_0 + \beta^{-1}\int_0^\infty d\upsilon\, S(\upsilon)W_E(\upsilon) \tag{13a}$$

$$S_{vib} = k\int_0^\infty d\upsilon\, S(\upsilon)W_S(\upsilon) \tag{13b}$$

$$A_{vib} = V_0 + \beta^{-1}\int_0^\infty d\upsilon\, S(\upsilon)W_A(\upsilon) \tag{13c}$$

where the weighting functions are

$$W_E(\upsilon) = \frac{\beta h\upsilon}{2} + \frac{\beta h\upsilon}{\exp(\beta h\upsilon) - 1} \tag{14a}$$

$$W_S(\upsilon) = \frac{\beta h\upsilon}{\exp(\beta h\upsilon) - 1} - \ln[1 - \exp(-\beta h\upsilon)] \tag{14b}$$

$$W_A(\upsilon) = \ln\left(\frac{1 - \exp(\beta h\upsilon)}{\exp(-\beta h\upsilon/2)}\right) \tag{14c}$$

2.4. Reference State and Reference Energy. For convenience, the reference energy V_0 is chosen in a way such that the reference state is the same as that calculated from the interaction force fields used in MD simulation. This is done by equating the total energy, E^{MD}, obtained from a molecular dynamics simulation to the energy, E^C, of the system when treating the vibrations classically, i.e.,

$$V_0 = E^{MD} - E^C \tag{15}$$

where

$$E^C = kT^2\frac{\partial}{\partial T}\ln q_{vib}^C = kT^2\frac{\partial}{\partial T}\int_0^\infty d\upsilon S(\upsilon) \ln q_{HO}^C(\upsilon) = kT\int_0^\infty d\upsilon\, S(\upsilon) \tag{16}$$

with $q_{HO}^C(\upsilon) = kT/(h\upsilon)$.

3. Molecular Dynamics Simulation

The molecular dynamics software Cerius2[21] is used to build the molecular structures and perform molecular dynamics

simulations. The Dreiding force field[22] is used to describe the valence and nonbond interactions, in which the total energy (E_{total}) of the system is composed of the following components

$$E_{total} = E_b + E_\theta + E_\phi + E_{inversion} + E_{vdW} + E_{Coulomb} \quad (17)$$

where E_b is the bond stretching energy, E_θ is the valence angle bending energy, E_ϕ is the dihedral angle torsion energy, $E_{inversion}$ is the inversion energy, E_{vdW} is the van der Waals interaction energy, and $E_{Coulomb}$ is the Coulombic interaction energy. Details of the energy function are found in the work by Mayo et al.[22] Nonbond energies (E_{vdW} and $E_{Coulomb}$) are calculated for all possible pairs, i.e., no cutoffs were applied.

For all the generations from core to generation 4, the linear and the circular hexamer aggregates are constructed using the 3-D Sketcher in Cerius2. The atomic charges for each monomer are calculated by the charge equilibration (QEq) method,[23] and energy minimization is then performed. This procedure of combining the charge equilibration and energy minimization is repeated 5 times. Out of the structures obtained from this procedure, the lowest energy structure is selected for the subsequent annealing process. In order to accelerate equilibration of the initial structures, an annealing process consisting of 10 cycles of NVT MD simulation at 600 K for 1 ps (using a 1 fs integration step), each followed by an energy minimization, is performed. The atoms in the core part of the dendrimer are fixed during the high-temperature (600 K) annealing process to prevent the aggregate from dissociating. The equilibration of structures finally is achieved by performing a second annealing process: 10 cycles of NVT dynamics at 300 K each for 1 ps and a subsequent energy minimization without any constraints on the molecule. All of the 10 structures from the previous annealing procedure, except for generation 4 where only three structures are used, are then chosen for 5 ps NVT equilibration followed by 20 ps NVT simulations (velocities, coordinates, and energies saved every 4 fs) at 300 K for data collection.

The vibrational contributions are determined using Fourier transform of the velocity autocorrelation function, which is calculated using the 20 ps equilibrium part of the trajectory with the maximum correlation time set to 10 ps. Fast Fourier transform is then performed to obtain the velocity spectrum $S(\upsilon)$. Together with the reference energy V_0 calculated from eq 15, the vibrational contributions can be determined from eq 13. It is important to note that the atomic velocity information has to be stored every 4 fs to prevent aliasing problems[24] in the velocity spectrum $S(\upsilon)$. [In discrete Fourier transform the Nyquist critical frequency υ_c (maximum frequency) is determined by the sampling intervals Δt as $\upsilon_c = 1/(2c\Delta t)$,[24] where c is the speed of light. A saving frequency of every 4 fs would lead to $\upsilon_c = 1/(2 \times 3 \times 10^{10} \times 4 \times 10^{-15}) = 4167\ cm^{-1}$. Furthermore, the resolution υ_m in $S(\upsilon)$ (minimum frequency) is determined by the length of the maximum correlation time T as $\upsilon_m = 1/(2cT)$. We have applied the windowing and window correction technique described in ref 25 which extends the correlation length by 50%. A 10 ps correlation time therefore results in a resolution of $\upsilon_m = 1/(2 \times 3 \times 10^{10} \times 10 \times 10^{-12} \times 1.5) = 1.1\ cm^{-1}$ in $S(\upsilon)$.] The principal moments of inertia of each dendrimer are determined from the atomic coordinates at every 4 fs. The instantaneous rotational properties are then calculated using eqs 2−4 and 6 with the symmetry number σ set to unity. The overall rotational contributions are averages over the 20 ps runs. The translational contribution is evaluated at one atmosphere and is a constant for dendrimers of the same molecular weight.

It is worth discussing our choice of 20 ps as the length of the thermodynamic analysis. We have separately performed simulations up to 100 ps (see the Appendix) and found that the total energy and entropy converge rapidly for circular-type dendrimers but quite slowly for linear conformations, especially at higher generations. We discovered that the slow convergence of the linear-type dendrimers is a result of dissociation (from the ends), which may occur as early as 40 ps of MD simulations. This is a clear indication of the instability of the linear dendrimers at longer times. Since we are interested in the relative stability of the dendrimers in different conformations, we chose to determine their thermodynamic properties from several independent 20 ps runs where the samples are still locally stable.

4. Results and Discussion

4.1. Structure and Thermodynamic Stability of the Dendrimer Core and Dendron. The core structure (Figure 1a) of the dendrimer has two isophthalic acid groups attached to the 2 and 12 position of a 7-*p*-(methoxy)phenyl-5,6,8,9-tetrahydrobenz[*c*,*h*]acridine group. The conformation of the core is characterized by two factors. One is the angle (ϕ) between the plane defined by the acridine group and the plane defined by the phenyl ring in the isophthalic groups; the other is the orientation of hydrogen in the carboxylic acid group. Figure 2 shows the conformation of the circular and linear core dendrimers at $\phi = 90°$ (upright form, Figure 2a and c) and $\phi = 31°$ (tilted form, Figure 2b and d). The upright form has a slightly smaller inner ring diameter (14.8 Å vs 15.3 Å) but more than a 2 times larger thickness (7.0 Å vs 3.3 Å) than the tilted form. The potential energy of the tilted form is found to be considerably lower than that of the upright form (256 kcal/mol vs 446 kcal/mol for circular hexamer; 313 kcal/mol vs 464 kcal/mol for linear aggregate). The titled core structure considerably reduces the unfavorable electrostatic repulsions observed in the upright form and also maximizes the favorable van der Waals interactions. Hence, the tilted core structure with the tilt angle $\phi = 31°$ is the most stable form of the core. Thus, in our studies we focused solely on the tilted forms for both the circular and linear configurations.

The orientations of the four carboxylic acid groups also lead to distinct core conformers. Figure 3 shows all of the 10 possible conformations ($2^4 = 16$, but 6 pairs are identical by symmetry, 180° of rotation of the molecule) in the tilted structure. Since the acid groups have to orient properly in order to form four hydrogen bond pairs between two monomers, not all combinations of the 10 conformers (labeled from a to j) are possible for the formation of aggregates. In Table 1, we compare the free energy of seven possible combinations that lead to circular and linear suprastructures. If only one type of monomer is allowed in the hexamer, only four conformations are able to form an aggregate for either the circular (all d, all e, all f, and all g) or the linear (all a, all d, all e, and all j) structures. These types of structures are named unimolecular hexamers. We have also studied all the possible conformations that contain two types of monomers in the hexamer: (a and j), (b and h), and (c and i) for the circular structures; (b and c), (f and g), and (h and i) for the linear structures. These types of structures are named bimolecular hexamers. Higher monomer-types-containing structures are possible but are not considered here. In general, the free energies are quite similar among the conformers (the maximum free energy difference is only 4% of the total free energy). The lowest free energy structures are found in the unimolecular hexamers for both the circular hexamer with the f-type monomer and the linear hexamer with the a-type

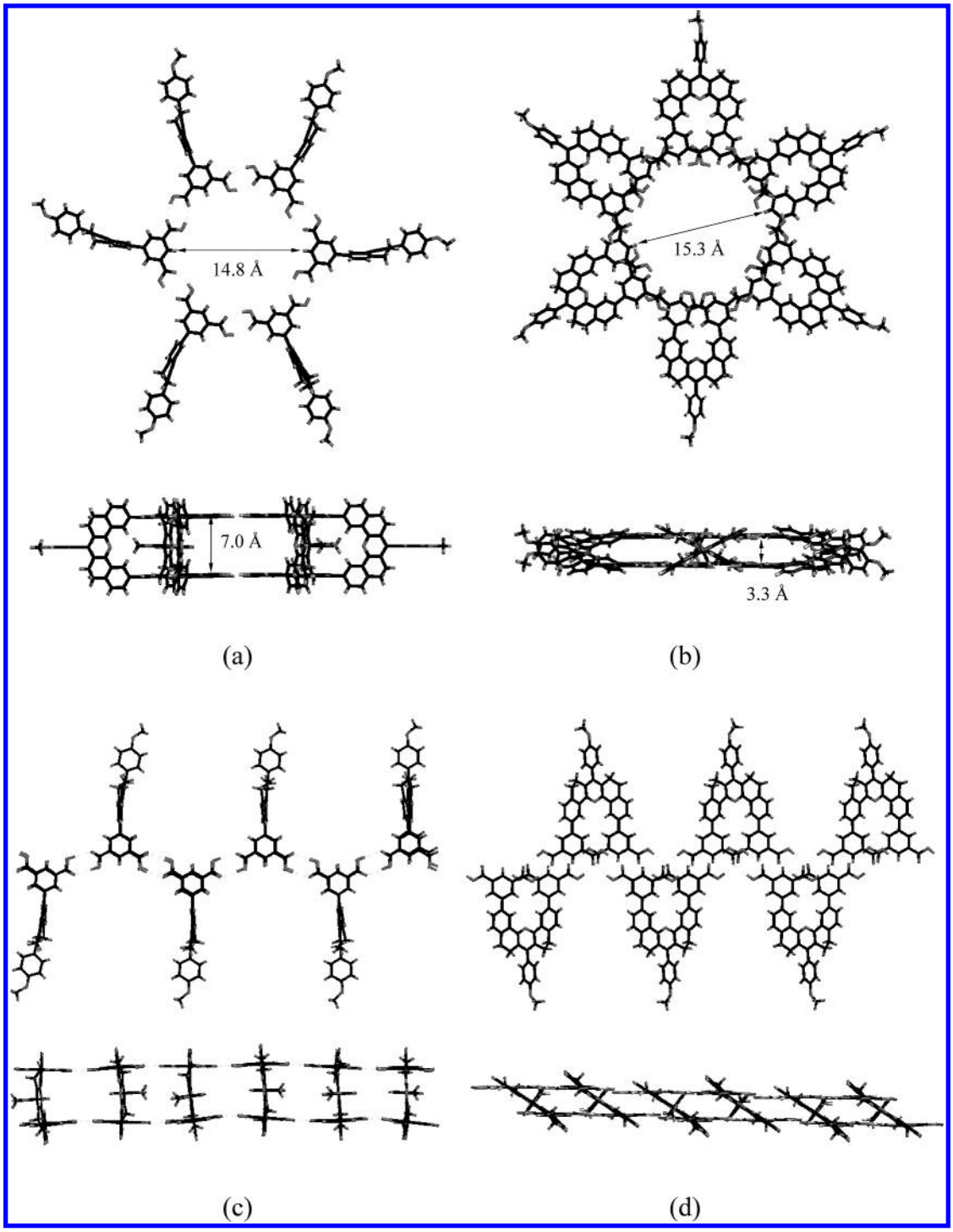

Figure 2. Upright form and tilted form for circular hexamer (a and b) and for linear aggregate (c and d).

monomer. For the core hexamers, the lowest free energy conformers coincide with the lowest energy ones. Thus, the determining factor of stability is mainly the enthalpic forces in these cases. We use the lowest free energy core conformations for the study of higher generation dendrimers.

The minimum energy structures of the dendron at different generations are shown in Figure 1d. These dendrons are poly(phenyl ether) compounds containing 3 ($= 1 + 2^1$), 7 ($= 3 + 2^2$), 15 ($= 7 + 2^3$), and 31 ($= 15 + 2^4$) phenyl ether groups from generations 1, 2, 3, and 4, respectively. The dendrons have planar, sector-like structures. As the number of phenyl ether groups increases rapidly, starting from generation 3, the minimum energy structures reveal stacking of the phenylene rings in order to lower the energy and stabilize the structures (Figure 1d). We have used these minimum energy configurations as the initial structures for all the molecular dynamics simulations to reduce the bias from using any amorphous initial structures.

4.2. Thermodynamic Stability of Higher Dendrimer Generations. The results of the thermodynamic analysis from the molecular dynamic simulations for the circular- and linear-type Zimmerman dendrimers at various generations (core to generation 4) are listed in Table 2. The free energy difference between the linear and circular forms indicates that the circular forms are relatively more stable for all generations. The difference comes to a minimum at generation 1 and increases rapidly after generation 2. Therefore, within the uncertainty, our simulation results show that both the linear and circular forms may coexist

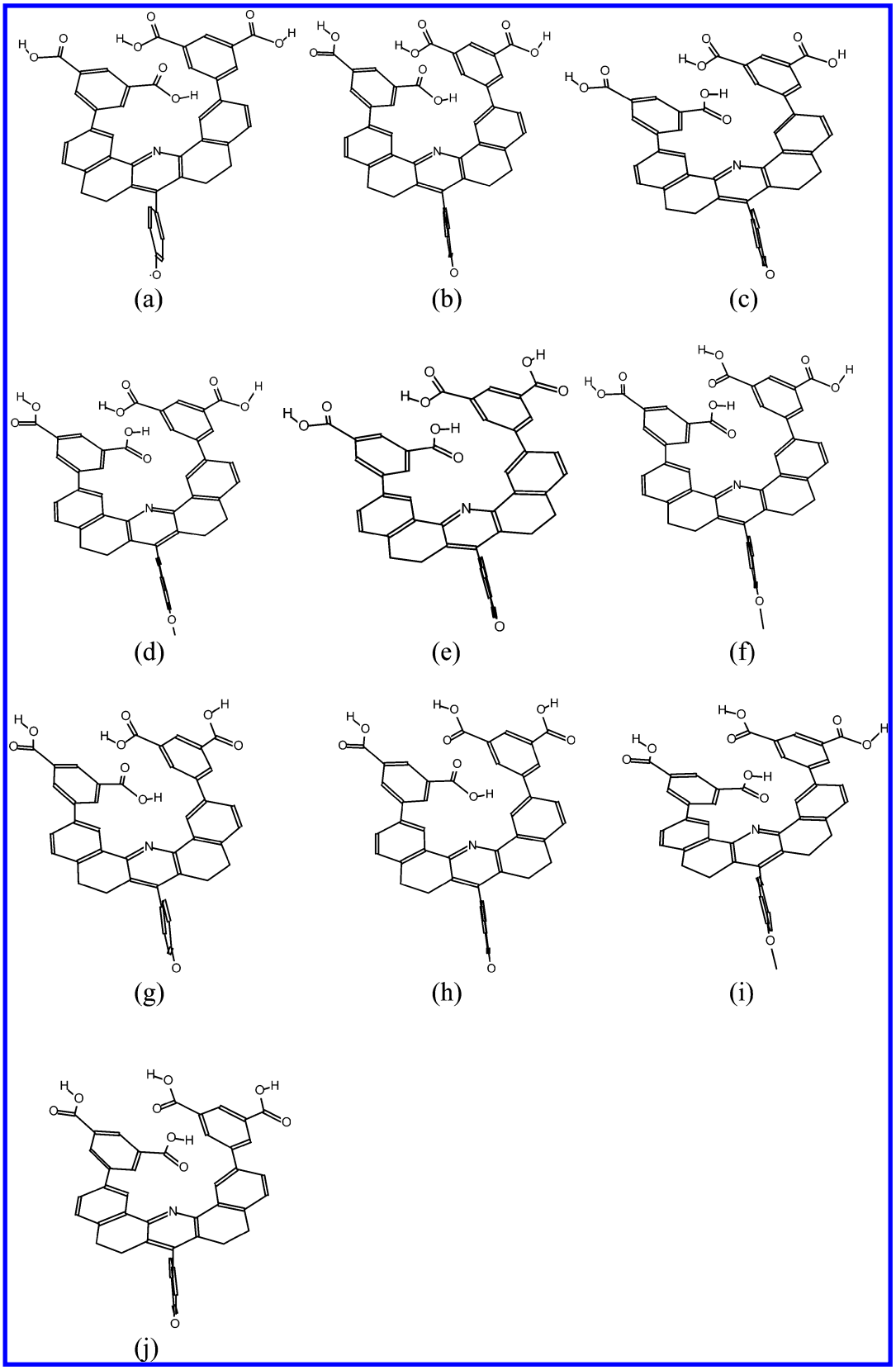

Figure 3. Ten possible monomer conformations as a result of different acid group orientation in the tilted ($\phi = 31°$) core dendrimers.

to up to generation 2 but the circular form is considerably more stable at higher generations. This is consistent with the experimental finding that circular and linear forms coexist in solution for generation 1 but only circular forms for generation 2 and higher.[16] The somewhat pronounced free energy for the core dendrimer compared to generation 1 is a result of parallel alignment of carbonyl groups in monomer type a (Figure 3a), which is the constituent monomer of the linear type, leading to unfavorable electrostatic repulsive interactions. The electrostatic energy difference between the monomers a and f due to the carbonyl group alignment is about 63 kJ/mol for the monomer, or 380 kJ/mol for the hexamer.

The driving force for the stability of the various suprastructures can be understood from a more detailed study on the

TABLE 1: Helmholtz Free Energy of Seven Possible Unimolecular or Bimolecular Hexamers of the Circular and the Linear Core Structure

	circular hexamer						
monomers	d	e	f[a]	g	a and j	b and h	c and i
A (kJ/mol)	10566	10644	10531	10942	10681	10878	10644
E (kJ/mol)	12361	12493	12301	12658	12457	12571	12398
TS (kJ/mol)	1794	1849	1770	1716	1775	1693	1755
	linear hexamer						
monomers	a[a]	d	e	j	b and c	f and g	h and i
A (kJ/mol)	10508	10659	10674	10673	10759	10854	10647
E (kJ/mol)	12466	12656	12621	12637	12711	12705	12607
TS (kJ/mol)	1958	1997	1947	1964	1953	1850	1959

[a] Most stable (lowest free energy) conformation.

TABLE 2: Comparison of Thermodynamic Stability between Circular and Linear Dendrimers at Various Generations[a]

generation	core	1	2	3	4
number of atoms	510	1026	1650	2898	5394
		A (kJ/mol)			
circular	10642	16466	23993	38934	68748
	(224)	(285)	(254)	(507)	(1107)
linear	10846	16627	24157	40072	71348
	(210)	(312)	(508)	(527)	(1557)
difference[b]	204	161	165	1139	2600
		E (kJ/mol)			
circular	12398	20192	29839	49124	86910
	(155)	(176)	(150)	(282)	(674)
linear	12714	20452	29998	49477	87874
	(159)	(189)	(332)	(341)	(904)
difference[b]	317	260	159	353	963
		TS (kJ/mol)			
circular	1756	3727	5847	10190	18162
	(77)	(139)	(174)	(242)	(1046)
linear	1868	3825	5841	9405	16526
	(72)	(134)	(199)	(228)	(668)
difference[b]	112	99	−6	−786	−1637
		E^{ZPE} (kJ/mol)[c]			
circular	10550	22033	35994	63830	120313
	(182)	(187)	(175)	(340)	(821)
linear	10425	21959	35932	64523	121969
	(173)	(231)	(357)	(449)	(1248)
difference[b]	−124	−74	−62	693	1656
		E^{MD} (kJ/mol)[d]			
circular	4831	4155	3516	2288	−1613
	(3)	(40)	(81)	(45)	(644)
linear	5246	4470	3723	2082	−1983
	(14)	(38)	(66)	(96)	(170)
difference[b]	416	314	206	−206	−369

[a] Numbers in parentheses represent the standard deviation. [b] Difference = linear − circular. [c] E^{ZPE}: zero-point energy. [d] E^{MD}: molecular dynamics energy (potential and kinetic).

energy and entropy listed in Table 2 and Figure 4. While the energy differences between the circular and the linear forms seem to be weakly dependent on the generation number and the entropy differences decrease rapidly with increasing generation, it is clear that the stability is driven by the entropic contribution. Considering that motions of suprastructures with low frequencies mainly contribute to the entropy, the entropy difference between different suprastructures can be regarded as a difference of structural flexibility represented by the low-frequency modes. The positive entropy differences between the linear and circular forms for the core and generation 1 dendrimers imply that the circular form is more rigid than the linear one. This is because the circular form has a closed

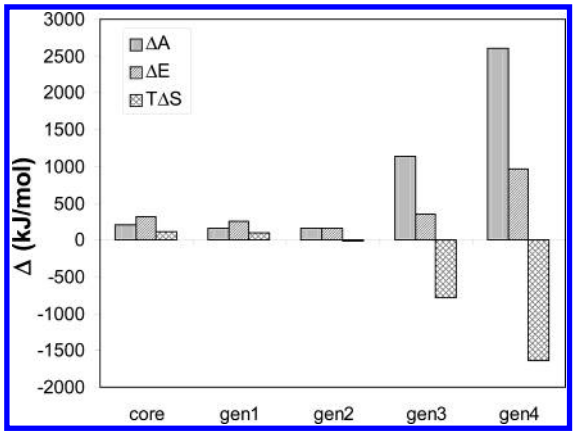

Figure 4. Relative (linear − circular) stability of the circular and linear dendrimers' conformations at different generations.

structure (all 24 hydrogen bond pairs are formed), whereas the linear form has an open structure in which two ends have four H-bond donors and four H-bond acceptors left unpaired. In contrast, at higher generation, the size of the dendrons takes a dominant role in determining the rigidity of the system. In other words, the available free space for dendrons in the linear form is more restricted by the neighboring dendrons than that in the circular form. Consequently, the dendrons in the linear form come in close contact at higher generations, leading to a more rigid conformation, whereas the circular conformation is relatively more flexible due to the larger free space available to the dendrons (Figure 5). Another evidence of the rigidity of the molecules is shown in the difference of the zero-point energies (ZPE) listed in Table 2. In contrast to entropy, zero-point energy is dominated by high-frequency modes. A larger value of ZPE in the self-assembled structure means that the structure is tightly packed or more strongly bound to each other. The ZPE of the circular form is smaller than that of the linear one for core to generation 2 but is larger for higher generations. These observations are consistent with our previous entropy-based explanation.

To analyze the change of thermodynamic stability with the increase of generation number, we determined the incremental thermodynamic properties from generation $(n - 1)$ to n as follows

$$\Delta P_{n,n-1} = \frac{P_n - P_{n-1}}{N_n - N_{n-1}} \tag{18}$$

where P_n and N_n are a property of interest and number of atoms, respectively, for generation n. The incremental property ($\Delta P_{n,n-1}$) is an indication of the change of a thermodynamic property as a result of introducing the last generation atoms. For the circular form, the incremental energy, entropy, and free energy are relatively insensitive to the generation number. For the linear form, however, the incremental free energy increases from 11.2 to 12.8 kJ/mol atom from generation 1 to generation 3 and then slightly decreases to 12.5 kJ/mol atom for generation 4. This is an indication that the packing of dendrons for the linear form is strongly generation dependent. The (temperature-weighted) incremental entropy of the linear form is quite similar to that of the circular form (3.8 kJ/mol atom) at low generations but decreases to 2.9 kJ/mol atoms at other generations while that of the circular form remains at about 3.5. This is a more strong evidence that the dendron packing in the linear form is significantly more rigid compared to that of the circular form from generation 2 and higher.

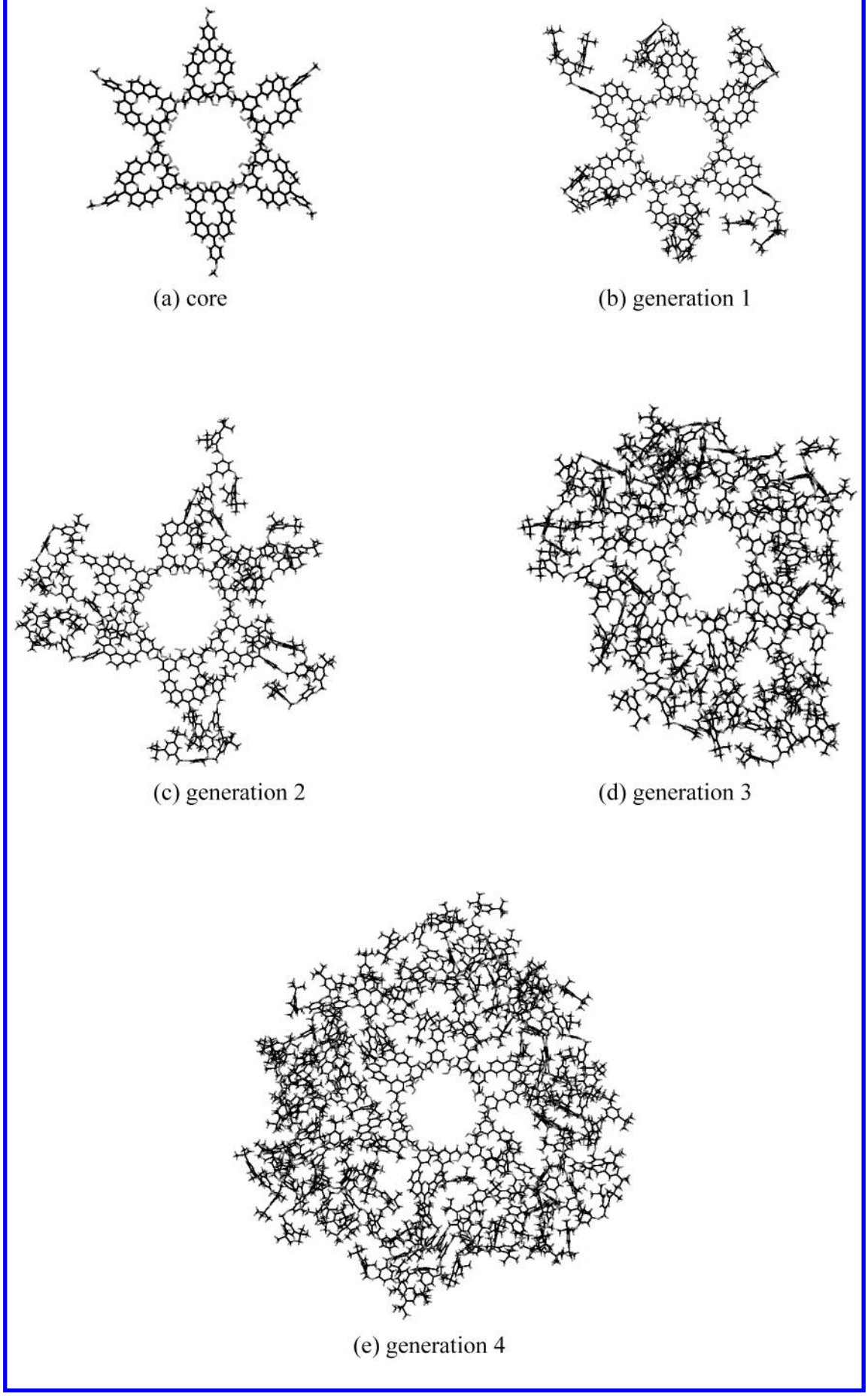

(a) core

(b) generation 1

(c) generation 2

(d) generation 3

(e) generation 4

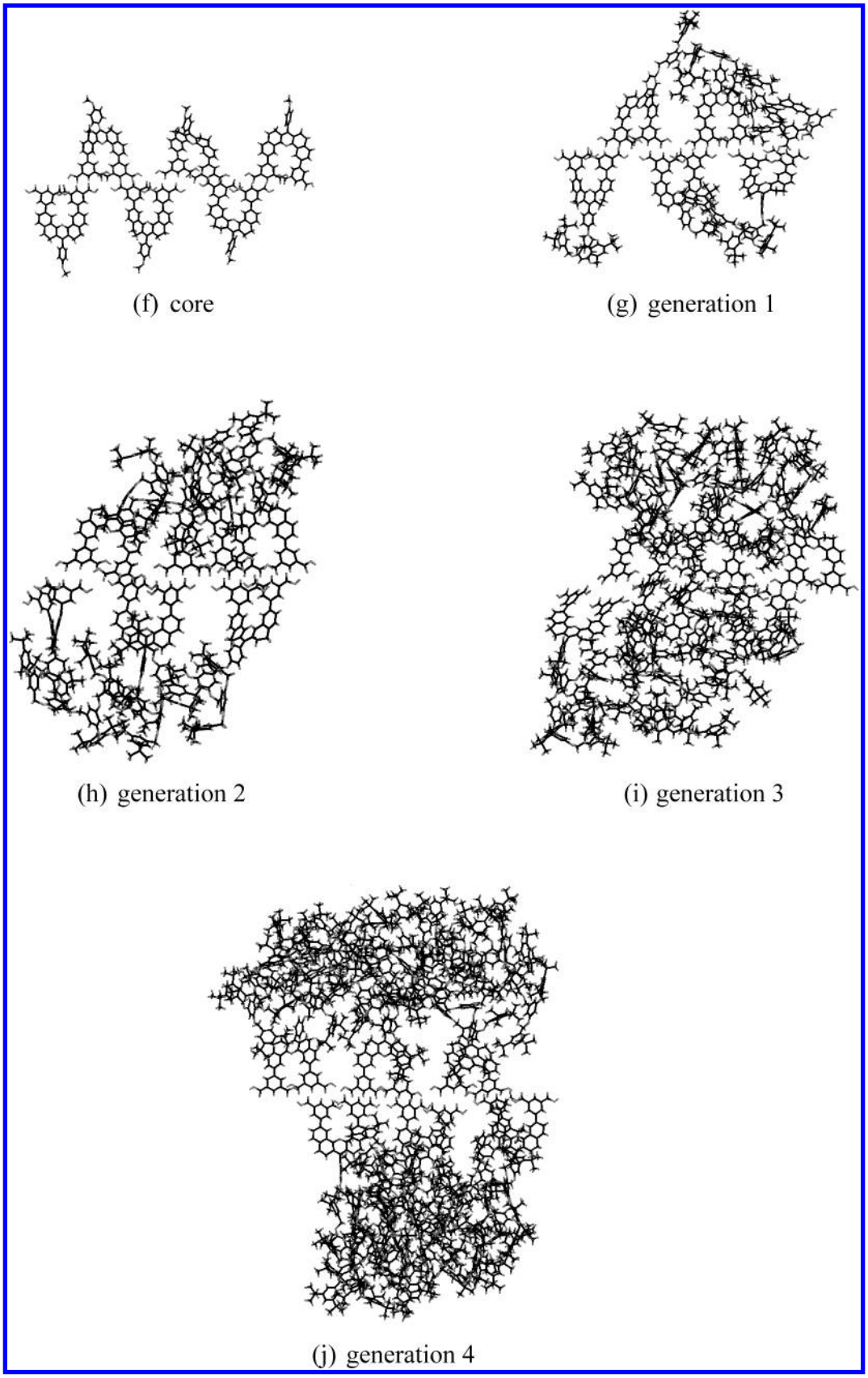

Figure 5. Molecular dynamics equilibrated structures of the Zimmerman H-bond dendrimers.

The molecular dynamics (MD) energy, i.e., the sum of the kinetic energy and the potential energy, is a measure for the strength of the interaction between monomers. We found that the total MD energy (Table 2) decreases with increasing generation number, meaning that the dendrons are favorably interacting through van der Waals and electrostatic interactions. It is noteworthy that the MD energy of the linear forms decreases faster than that of the circular form as the generation number is increased, and thus, the linear form is enthalpically favorable at higher generations.

TABLE 3: Comparison of Incremental Thermodynamic Properties between Circular and Linear Dendrimers at Various Generations

generation	1	2	3	4
increase of atoms[a]	516	624	1248	2496
	$\Delta A_{n,n-1}$ (kJ/mol atom)[b]			
circular	11.3	12.1	12.0	11.9
linear	11.2	12.1	12.8	12.5
difference[c]	−0.1	0.0	0.8	0.6
	$\Delta E_{n,n-1}$ (kJ/mol atom)[b]			
circular	15.1	15.5	15.5	15.1
linear	15.0	15.3	15.6	15.4
difference[c]	−0.1	−0.2	0.2	0.2
	$T\Delta S_{n,n-1}$ (kJ/mol atom)[b]			
circular	3.8	3.4	3.5	3.2
linear	3.8	3.2	2.9	2.9
difference[c]	0.0	−0.2	−0.6	−0.3
	$\Delta E^{ZPE}_{n,n-1}$ (kJ/mol atom)[b]			
circular	22.3	22.4	22.3	22.6
linear	22.4	22.4	22.9	23.0
difference[c]	0.1	0.0	0.6	0.4
	$\Delta E^{MD}_{n,n-1}$ (kJ/mol atom)[b]			
circular	−1.3	−1.0	−1.0	−1.6
linear	−1.5	−1.2	−1.3	−1.6
difference[c]	−0.2	−0.2	−0.3	−0.1

[a] Increase of number of atoms from previous generation, i.e., (total number of atoms in generation n) − (total number of atom in generation $n-1$). [b] Increase of thermodynamic property per atom, i.e., eq 18. [c] Difference = linear − circular.

Furthermore, the incremental MD energies (Table 3) are all negative, suggesting that the van der Waals attraction is still dominant and the steric effect (due to van der Waals repulsions) is not significant even up to generation 4. This is in contrast to the previous reasoning that attributes the lower stability of the linear form to the "unfavorable steric repulsion between proximal dendrimers."[16] In fact, the stronger van der Waals interactions in the linear form may lead to a more rigid structure, resulting in a decrease of entropy and an increase of free energy.

The density of state (DoS) distributions of both the circular and the linear forms at various generations are shown in Figure 6. Because of the identical chemical ingredients in the supramolecules, their DoS distributions are quite similar, especially in the mid- to high-frequency domain. The increase of generation number significantly increases the populations in the low-frequency regime, e.g., $\nu < 500$ cm^{-1}. This indicates that the dendrons behave as flexible sectors up to generation 4. The integration of the density of state distribution (Figure 7) in the low-frequency regime is a more direct assessment of the flexibility of the dendrimers. It is found that circular structures have less modes populates below 30 wavenumbers up to generation 2. The situation is reversed for generations 3 and 4. Therefore, at lower generation, in which the role of the core is more important in determining the stability in comparison with the dendron, the circular form is rigid. At higher generation, in which the dendron becomes important, the linear form is rigid because of compact packing of the dendron.

4.3. Binding Energy of Dendrimer at Various Generations. The binding free energies, $\Delta A_{bind} = A_{hexamer} - 6A_{monomer}$, in the circular and linear forms for various generation dendrimers are listed in Table 4. Both the circular and linear forms are favored in the aggregated forms as indicated by the negative values of ΔA_{bind}. The increasing difference in the binding free energy with generation number between the two configurations suggests that the circular forms are preferred at high generations. This is consistent with the experimental observation and

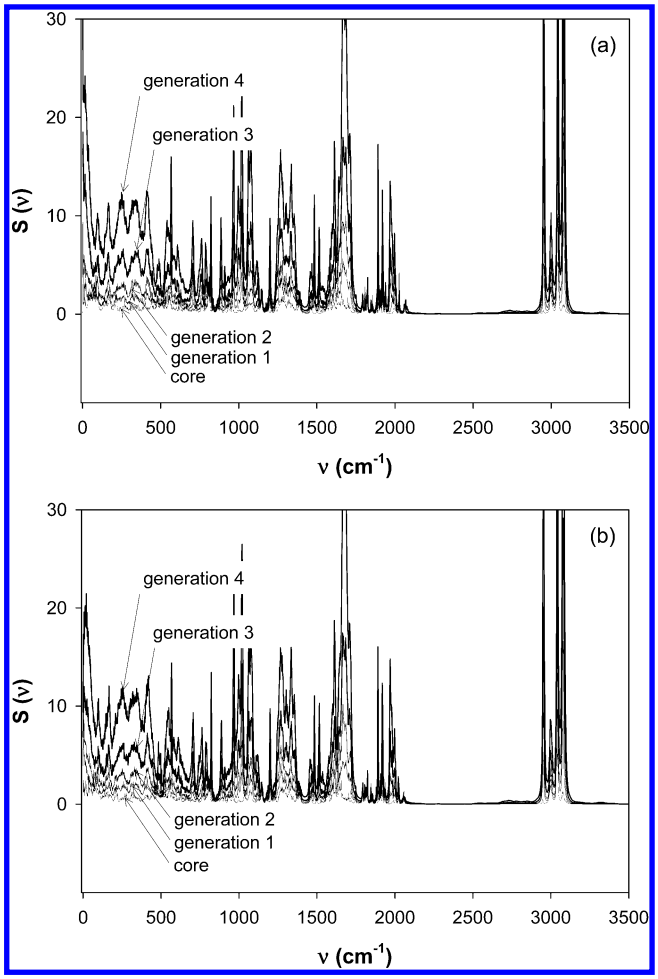

Figure 6. Velocity spectrum of circular (a) and linear (b) dendrimers at various generations.

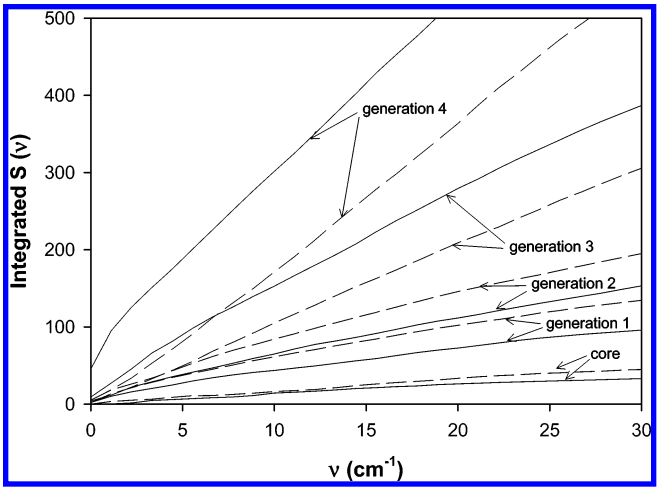

Figure 7. Plot of the integrated density of state for the circular (solid line) and linear (dashed line) dendrimers.

previous stability analysis. It is found that there is a stronger generation dependence in the difference of the binding entropy, $\Delta\Delta S_{bind}$, while such dependency is much weaker in the binding potential energy, $\Delta\Delta E_{bind}$. The positive differences in ΔS_{bind} for the core and first generation dendrimer indicate the enhancement of entropy in the formation of linear-type structures. On the contrary, for generation 2 and higher the difference in ΔS_{bind} becomes negative. This can, again, be attributed to the change of structural rigidity as a result of the competition between contributions of the core part and the dendron part. For core

TABLE 4: Energy, Entropy, and Free Energy of Binding for the Circular and Linear Type Dendrimers at Different Generations

energy		generation core	1	2	3	4
ΔA_{bind} (kJ/mol)	circular	−317	−2267	−3529	−5266	−8956
	linear	−113	−2106	−3365	−4127	−6356
	difference[a]	204	161	165	1139	2600
ΔE_{bind} (kJ/mol)	circular	−632	−1854	−2422	−3369	−5760
	linear	−316	−1594	−2264	−3016	−4797
	difference[a]	317	260	159	353	963
$T\Delta S_{bind}$ (kJ/mol)	circular	−315	407	1098	1882	3170
	linear	−204	505	1092	1098	1539
	difference[a]	112	99	−6	−783	−1631

[a] Difference = linear − circular.

and generation 1, the dendrimer's core conformation (circular or linear) dominates the stability of the supramolecule. While the circular form is energetically more stable, the linear form is entropically more favorable due to the flexibility of the free ends. The two effects cancel, and indeed both conformations are possible, i.e., can be observed experimentally. For higher generations, the dendrons play a more important role. Although the close packing of dendrons in the linear form results in a favorable van der Waals interaction, the overall binding free energy is overwhelmed by the low entropy and high zero-point energy due to the rigidity of the close-packed dendrons.

5. Summary and Conclusions

We have utilized the velocity spectrum method of Berens et al.[17] to extract free energies directly from classical molecular dynamics (MD) simulations to investigate the origin of the generation-dependent stability of the hydrogen-bond-mediated self-assembly of the supramolecular hydrogen-bond-mediated dendrimers synthesized and characterized by Zimmerman and co-workers. Our simulation results confirm the experimental findings that circular and linear configurations may coexist at lower generations but that only circular forms are stable at higher generations.

Which structure is stabile is determined by the competition between enthalpic and entropic forces at each generation. For low-generation dendrimers, i.e., core and generation 1, the strong binding in the circular conformations balances with the entropically favorable flexible linear structures. Therefore, the two forms coexist. For higher generations, i.e., generations 2−4, the large dendron portion begins to dominate the stability of the suprastructure. The limited space available to the dendrons in the linear form results in a close packing of dendrons. *Steric hindrance effects are not yet important even at generation 4*, and the close packing of dendrons are enthaplically favorable through van der Waals attraction. However, the close-packed structure has significantly lower entropy and higher zero-point energy contributions, resulting in a higher free energy for the linear structures. Consequently, *the more flexible circular conformations gain increased stability at high generations.* We expect that at generation 5 or higher, steric effects may begin to play a more important role and that the linear structure would become unfavorable for enthalpic reasons in addition to entropy.

This work explored the generation dependence of H-bond-mediated dendrimers in vacuum, or equivalently, in the most apolar solvent condition. We find good qualitative agreement with experiment on the relative stability of the circular and linear suprastructures, however, we predict a much stronger stability of the circular form at low generation in the most apolar solvent condition as compared to the experiments which are done with moderately apolar solvents such as dichloromethane. We expect that the use of more realistic solvents would decrease the differences between the linear and circular forms at lower generations. Quantitative agreement with experiment on the SEC measurements can be expected once solvent effects are included. Work is now in progress in this direction.

We expect that the understanding of other complex suprastructures such as proteins and DNA could also benefit from the detailed information about the thermodynamic properties extracted from MD simulations

Acknowledgment. This material is based upon work supported in part by the U.S. Army Research Laboratory and the U.S. Army Research Office under Grant No. DAAG55-97-1-0126. Other parts of this research were supported by an NSF-NIRT. The facilities of the MSC are also supported by Grants from NSF-MRI, ARO (DURIP), ONR (DURIP), Chevron-Texaco, General Motors, Seiko Epson, Asahi Kasei, and the Beckman Institute.

Appendix

Figure A1 shows the time variation in total MD energy (kinetic plus potential) and entropy for Zimmerman H-bond dendrimers up to generation 2. The data are collected from a single MD run of 100 ps for each of the dendrimers. The error bars shown at 50, 25, 12.5, and 6.25 ps are analyzed from partitioning the 100 ps trajectory into 2, 4, 8, and 16 equal length fragments. It is found that the properties of circular-type

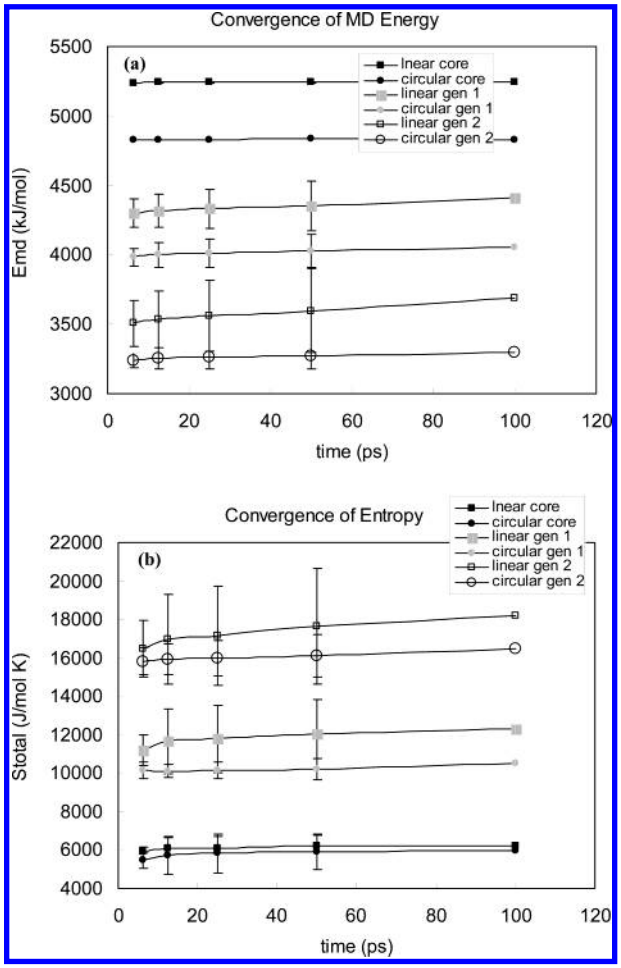

Figure A1. Time evolution in energy (a) and entropy (b) for Zimmerman H-bond dendrimers.

dendrimers and the core of the linear type converge quickly, whereas those of the linear-type generations 1 and 2 continue to vary even up to 100 ps. The relatively larger standard deviation for the linear-type structures and its slow convergence in energy and entropy indicate that an equilibrium structure is not reached. From a visual examination of the structure evolutions we found that the linear forms start to dissociate (starting from the two ends) as early as after 40 ps of MD simulations. This is another clear indication of the instability of the linear form and also the reason for the choice of 20 ps to access the local thermodynamic properties of the dendrimers.

References and Notes

(1) Watson, J. D.; Crick, F. H. C. *Nature* **1953**, *171*, 737.
(2) Dickerson, R. E.; Geis, I. *Hemoglobin: Structure, Function, Evolution, and Pathology*; Benjamin Cumming Publishing Co.: Reading, MA, 1983.
(3) Westhof, E.; Leontis, N. *Angew. Chem., Int. Ed.* **2000**, *39* (9), 1587.
(4) Lehn, J.-M. *Angew. Chem., Int. Ed. Engl.* **1988**, *27*, 89.
(5) Zimmerman, S. C.; Corbin, P. S. *Struct. Bonding* **2000**, *96*, 63.
(6) Lawrence, D. S.; Jiang, T.; Levett, M. *Chem. Rev.* **1995**, *95*, 2229.
(7) Whitesides, G. M.; Mathias, J. P.; Seto, C. T. *Science* **1991**, *254*, 1312.
(8) Philip, D.; Stoddart, J. F. *Angew. Chem., Int. Ed. Engl.* **1996**, *35*, 1154.
(9) Lindsey, J. S. *New J. Chem.* **1991**, *15*, 153.
(10) Niemeyer, C. M.; Adler, M. *Angew. Chem., Int. Ed.* **2002**, *41* (20), 3779.
(11) Niemeyer, C. M. *Angew. Chem., Int. Ed.* **2001**, *40*, 4128.
(12) Mao, C.; Sun, W.; Shen, Z.; Seeman, N. C. *Nature* **1999**, *397*, 144.
(13) Seeman, N. C. *Angew. Chem., Int. Ed.* **1998**, *37*, 3220.
(14) Corbin, P. S.; Lawless, L. J.; Li, Z. T.; Ma, Y. G.; Witmer, M. J.; Zimmerman, S. C. *Proc. Natl. Acad. Sci. U.S.A.* **2002**, *99* (8), 5099.
(15) Zeng, F.; Zimmerman, S. C. *Chem. Rev.* **1997**, *97*, 1681.
(16) Zimmerman, S. C.; Zeng, F. W.; Reichert, D. E. C.; Kolotuchin, S. V. *Science* **1996**, *271* (5252), 1095.
(17) Berens, P. H.; Mackay, D. H. J.; White, G. M.; Wilson, K. R. *J. Chem. Phys.* **1983**, *79* (5), 2375.
(18) Karplus, M.; Kushick, J. N. *Macromolecules* **1981**, *14* (2), 325.
(19) Levy, R. M.; Karplus, M.; Kushick, J.; Perahia, D. *Macromolecules* **1984**, *17* (7), 1370.
(20) Lin, S. T.; Blanco, M.; Goddard, W. A., III. *J. Chem. Phys.* **2003**, *119* (22), 11792.
(21) *Cerius2 Modeling Environment*, release 4.0.; Accelrys Inc.: San Diego, CA, 1999.
(22) Mayo, S. L.; Olafson, B. D.; Goddard, W. A., III. *J. Phys. Chem.* **1990**, *94*, 8897.
(23) Rappe, A. K.; Goddard, W. A., III. *J. Phys. Chem.* **1991**, *95*, 3358.
(24) Press, W. H.; Flannery, B. P.; Teukolsky, S. A.; Vetterling, W. T. *Numerical Recipes—The Art of Scientific Computing*; Cambridge: New York, 1986.
(25) Berens, P. H.; Wilson, K. R. *J. Chem. Phys.* **1981**, *74* (9), 4872.